

Spin relaxation and coherence times for electrons at the Si/SiO₂ interface

S. Shankar,* A. M. Tyryshkin, Jianhua He, and S. A. Lyon
Dept. of Electrical Engineering, Princeton University, Princeton, NJ 08544, USA

While electron spins in silicon heterostructures make attractive qubits, little is known about the coherence of electrons at the Si/SiO₂ interface. We report spin relaxation (T_1) and coherence (T_2) times for mobile electrons and natural quantum dots at a ²⁸Si/SiO₂ interface. Mobile electrons have short T_1 and T_2 of 0.3 μ s at 5 K. In line with predictions, confining electrons and cooling increases T_1 to 0.8 ms at 350 mK. In contrast, T_2 for quantum dots is around 10 μ s at 350 mK, increasing to 30 μ s when the dot density is reduced by a factor of two. The quantum dot T_2 is shorter than T_1 , indicating that T_2 is not controlled by T_1 at 350 mK but is instead limited by an extrinsic mechanism. The evidence suggests that this extrinsic mechanism is an exchange interaction between electrons in neighboring dots.

PACS numbers: 73.20.-r; 76.30.-v

I. INTRODUCTION

Electron spins confined in quantum dots in silicon are a promising quantum computing architecture^{1,2} that builds on the substantial experience with scaling classical electronics. One challenge for these solid-state based qubits is that the spin relaxation (T_1) and coherence (T_2) times need to be much longer than the gate operation time, to ensure that errors do not destroy a computation³. Silicon based heterostructures are particularly advantageous in this regard since spins in silicon can potentially have long T_1 's and T_2 's. For example, extensive measurements have shown that electron spins bound to donors in bulk silicon have long relaxation times⁴, with coherence times reaching over 1 s at 1.8 K⁵. In contrast, only a few measurements of T_1 have been reported on spins confined in quantum dots in silicon^{6,7} while there have been no measurements of T_2 . Thus, for progress towards a practical technology, it is crucial to measure the T_1 and T_2 of spins confined in silicon quantum dots as well as to understand the mechanisms limiting them.

Here we perform electron spin resonance (ESR) experiments to measure the T_1 and T_2 of mobile 2D electrons as well as electrons confined in natural quantum dots in a silicon MOSFET. We find that mobile electrons at the Si/SiO₂ interface have a T_1 and T_2 of about 0.3 μ s at 5 K, shorter than for 2D electrons in Si/SiGe heterostructures⁸. As in Si/SiGe structures, spin relaxation may be controlled by a fluctuating Rashba effective magnetic field (B_{BR}) due to the spin-orbit interaction^{9,10}.

We have previously¹¹ shown that when the MOSFET gate voltage is lowered below threshold, the natural disorder at the Si/SiO₂ interface fortuitously confines electrons into isolated, independent dots with confinement energies of a few millivolts. While not obviously useful for quantum information processing, these natural dots provide a system to study spin decoherence processes that might affect gate defined quantum dots. Here we extend our previous experiments to show that T_1 for some of these natural dots increases rapidly with decreasing

temperature below 1 K, reaching 0.8 ms at 350 mK. Our results are consistent with theory¹² and other recent experiments in silicon^{6,7} showing that upon confinement and cooling to low temperature, the Rashba field is less effective in inducing the relaxation.

The longest T_2 measured for the natural dots is 30 μ s at 350 mK, two orders of magnitude longer than for mobile electrons but shorter than the T_1 of 0.8 ms. T_2 depends on the density of confined electrons, with shorter T_2 observed for higher dot densities. This observation suggests that exchange interactions between the dots is the limiting mechanism for T_2 which may explain why $T_2 \ll T_1$.

II. MATERIALS AND METHODS

A silicon n-channel accumulation MOSFET was fabricated on an isotopically enriched ²⁸Si epi-wafer having 800 ppm of ²⁹Si. The (100) oriented epilayer was 25 μ m thick and was doped with phosphorus to a density of 10^{14} cm⁻³. The MOSFET had a large gate area (0.4×2 cm²) in order to obtain adequate ESR signal from 2D electrons¹¹. The device consisted of phosphorus implanted source-drain contacts, a 110 nm dry thermal gate oxide, and a Ti/Au metal gate. Transport measurements at 4.2 K gave a threshold voltage of 1 V, an electron density of 2×10^{11} cm⁻² V⁻¹ and a peak Hall mobility of 14 000 cm² V⁻¹ s⁻¹.

Continuous wave (CW) and pulsed ESR experiments were performed using a commercial ESR spectrometer (Bruker Elexsys580) operating at X-band frequencies (9–10 GHz). A ³He cryostat (Janis Research) was used to maintain temperature down to 350 mK. The spin dephasing time (T_2^*) caused by static inhomogeneities was extracted from the linewidth measured in the CW ESR experiment. Standard pulse sequences were used to measure T_1 and T_2 ¹³. T_2 was measured using a 2-pulse Hahn echo sequence ($\pi/2 - \tau - \pi - \tau - \text{echo}$). T_1 was measured using a 3-pulse inversion recovery sequence comprising an initial inverting π pulse followed by a measurement sequence using 2-pulse echo detection ($\pi - t - \pi/2 - \tau -$

$\pi - \tau - \text{echo}$). Imperfections in the microwave pulses can contaminate Hahn echo and inversion recovery decays with extraneous signals that decay on a timescale of T_2^* . Therefore, a 16-step phase cycling sequence was used to remove these extraneous signals and measure the true T_2 and T_1 (Ref. 13, p. 133-135).

Microwave pulses of optimal power (520 ns π pulse length), were used to avoid electron heating. At higher powers, T_1 for natural dots decreases indicating some microwave heating. Unfortunately, below this power, the microwave magnetic field B_1 was smaller than the ESR linewidth (20 μT) resulting in reduced sensitivity. While we cannot rule out microwave heating at the lowest temperatures, the pronounced temperature dependence of T_1 suggests that residual heating is small.

III. RESULTS

The ESR spectra of the MOSFET reveal a gate voltage (V_G) dependent signal having a g-factor of 1.9999(1) arising from 2D electrons at the Si/SiO₂ interface, similar to that reported previously¹¹. When V_G is greater than the threshold voltage ($V_{th} = 1$ V) (the Fermi energy, E_F , above the conduction band edge, E_C), the signal corresponds to mobile 2D electrons in the conduction band. The signal magnitude is independent of V_G above V_{th} , consistent with a constant density of states, $g(E)$, of 2D electrons above E_C (Fig. 1(b)). On the other hand, when V_G is below V_{th} (i.e. $E_F \leq E_C$), the ESR signal corresponds to electrons confined in a disorder induced band tail of states below E_C (Fig. 1(b) and Ref. 14, p. 517). The signal below V_{th} exhibits a Curie susceptibility (inversely proportional to temperature) indicating that electrons in confined states behave as isolated spins¹¹. Hence, gate voltage control of our MOSFET conveniently allows ESR measurements under identical conditions on both mobile 2D electrons as well as isolated electrons confined in quantum dots.

Figure 1(a) illustrates a typical dependence of the ESR signal intensity, proportional to the number of unpaired electron spins (N_S) in the MOSFET, as a function of V_G . In these experiments, at each temperature, V_G was first biased at 2 V (i.e. above threshold) and then progressively reduced while measuring the spins. At 4.8 K when measured in the dark (squares), N_S decreases as V_G decreases, and then becomes constant at $V_G = 0.4$ V (marked as V_T^* in Fig. 1(a)). For V_G below 0.4 V in the dark, electrons are confined into dots with a characteristic depth greater than $k_B T$ (i.e. $E_C - E_F \gtrsim k_B T$, where k_B is the Boltzmann constant and T is the temperature), and are therefore unable to thermally escape to the source or drain contacts. Brief illumination neutralizes the dots so that N_S measured after illumination goes to zero at 0 V (circles). In contrast, at a lower temperature of 2 K (triangles), N_S becomes constant at a higher V_G of 0.6 V; the dots have a correspondingly shallower depth ($E_C - E_F \gtrsim 2$ K). Thus at any given temperature,

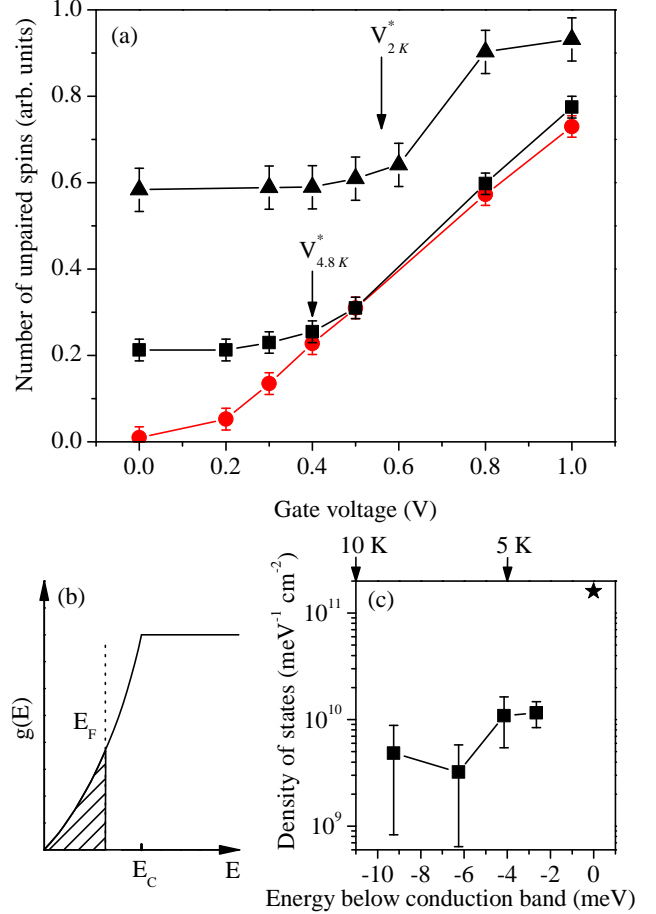


FIG. 1. (a) Number of unpaired spins (N_S) as a function of gate voltage (V_G) below threshold ($V_{th} = 1$ V) as measured at 4.8 K in the dark (squares) and after illumination (circles), and at 2 K in the dark (triangles). Arrows on the curves recorded in the dark indicate a characteristic voltage V_T^* at which N_S becomes constant while decreasing V_G from V_{th} . Lines are guides for the eye. (b) Cartoon of density of states, $g(E)$, of 2D electrons; $g(E)$ is constant above the conduction band edge (E_C) and decays below E_C . States below E_F are occupied. In the experiment, E_F can be adjusted by the gate voltage bias V_G . (c) Density of states of confined electrons as a function of energy below E_C , as obtained from data in Fig. 1(a). The star indicates the calculated value ($1.6 \times 10^{11} \text{ meV}^{-1} \text{ cm}^{-2}$) of the density of states in the conduction band for 2D electrons at a Si(100) surface (two-fold valley degeneracy). The labeled arrows on the top axis indicate the depth of confined electrons after setting $V_G = 0$ V in the dark at 5 K and 10 K, respectively.

by first biasing the gate above threshold and then reducing V_G to 0 V, we freeze electrons into natural quantum dots with a confinement depth characteristic of the temperature.

The characteristic gate voltages V_T^* at which N_S becomes constant were measured for several temperatures in the range from 2 K to 10 K. These V_T^* were then used

to estimate the energies and density of confined electron states below E_C . For each temperature, T , the total number of confined electrons was first calculated using the gate capacitance (2×10^{11} electrons/Vcm 2) and the corresponding measured V_T^* . Then, assuming that electrons are thermally activated, the characteristic confinement energy was calculated for that T^{15} . Finally, the ratio of the difference in the numbers of confined electrons to the difference in the confinement energies between any two temperatures gives the density of confined electron states. Our result for the density of states is shown in Fig. 1(c). Also shown for comparison is the density of states calculated for mobile 2D electrons at a (100) Si/SiO $_2$ surface (given by $g_v m / \pi \hbar^{214}$, where $g_v = 2$ is the valley degeneracy, m is the effective mass of the electron, and \hbar is the Planck's constant). As Fig. 1(c) indicates, natural quantum dots in our sample have characteristic confinement energies of a few millivolts.

Having determined the confinement energies of the natural quantum dots, pulsed ESR spectroscopy as a function of gate voltage and temperature was performed to determine T_1 and T_2 for both natural dots and mobile electrons at the Si/SiO $_2$ interface. Most pulsed measurements on quantum dots were done with dots confined at 5 K, i.e. V_G was first taken above threshold at 5 K and then brought back to 0 V leaving only electrons trapped deeper than about 4 meV (Fig. 1(c)). The device was then cooled to temperatures as low as 350 mK, freezing electrons into these confined states. A single T_2 experiment was also done on dots confined at 10 K, where the electrons are estimated to be trapped deeper than about 11 meV.

In the T_2 experiment, the magnetic field was swept during echo detection and a broad underlying baseline was subtracted in order to remove any echo signal contributed by background spins. Fig. 2(a) shows typical field-sweep spectra, obtained after removing baselines, of the echo intensity at the end of a 2-pulse sequence. The signal at about 366.7 mT ($g = 1.9999$) belongs to electrons at the Si/SiO $_2$ interface. The peak intensity of the signal is plotted as a function of time in Fig. 2(b), and the exponential fit gives T_2 . In some experiments on natural dots, such as the one shown in Fig. 2(b), the echo decays were non-exponential and best fitted using a bi-exponential function $(A_1 \exp \{-2\tau/T_2^{(1)}\} + A_2 \exp \{-2\tau/T_2^{(2)}\})$.

The bi-exponential decay arising from the natural dots is suggestive of a broad distribution of dots with a range of T_2 values. For example, for natural dots confined at 5 K shown in Fig. 2, approximately 90 % of the electrons have a short T_2 of 0.8 μ s while about 10 % show a longer T_2 of 9 μ s. A similar bi-exponential decay was observed for natural dots confined at 10 K (Fig. 3); as discussed below, confinement at 10 K reduces the total electron density by about a factor of two as compared to confinement at 5 K. As seen in Fig. 3, the natural dots confined at 10 K exhibit a similar fraction of dots showing a short T_2 of 0.9 μ s while the remainder show an even longer T_2

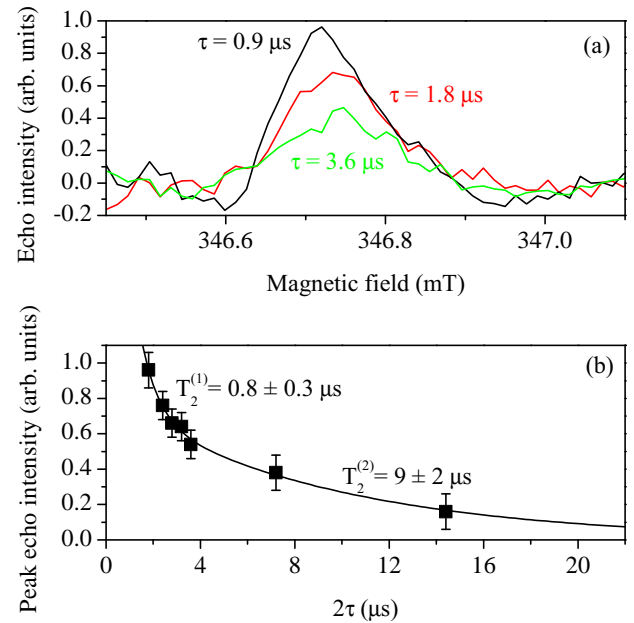


FIG. 2. T_2 experiment on electrons confined in dots at 5 K as measured at 350 mK. (a) Typical echo detected spectra after a two-pulse sequence for different τ . (b) Peak intensity of the 2-pulse signal as function of 2τ . The bi-exponential fit gives two characteristic T_2 's.

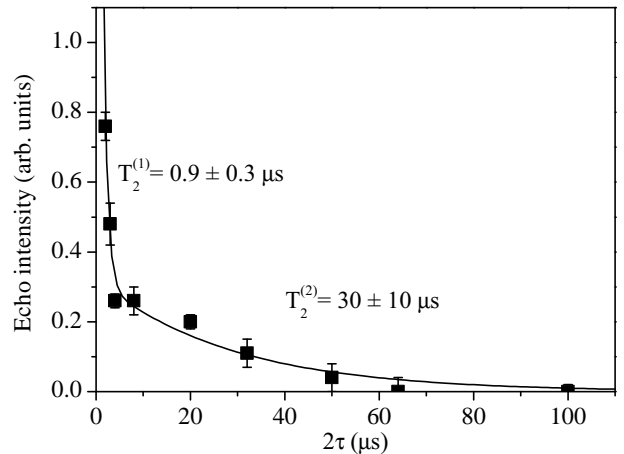


FIG. 3. 2-pulse echo decay for natural dots confined at 10 K, measured at 350 mK.

of 30 μ s. In Sec. IV, we propose that the bi-exponential echo decay and the dependence of T_2 on the confinement temperature indicates that T_2 for these natural dots is controlled by exchange interactions between neighboring dots. Since the distance between any two dots is random, there will be a broad distribution in the exchange interaction between dots. The broad distribution in exchange results in some dots decohering quickly (a short T_2), while others decohere slowly (a long T_2); thus the echo signal cannot be characterized by a single exponen-

TABLE I. Spin-counting results

Confinement temperature (K)	Density of dots in CW ESR (10^{10} cm^{-2})	Density of dots that show long T_2 (10^9 cm^{-2})
5	1.2	1.0
10	0.7	0.5

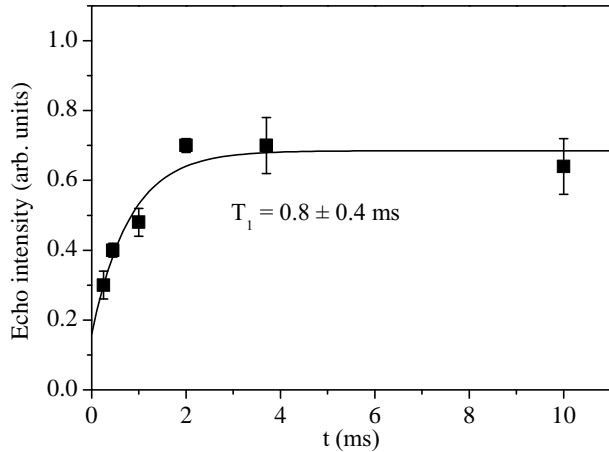


FIG. 4. Echo intensity at the end of the 3-pulse experiment on natural dots confined at 5 K and measured at 350 mK. The exponential fit of the intensity as a function of t gives T_1 .

tial decay.

We performed a spin-counting experiment in order to quantify the density of natural dots confined at 5 K and 10 K. These densities are used in Sec. IV to estimate the magnitude of the exchange interactions between neighboring dots. In the spin-counting experiment, the absolute density of electron spins in dots measured in both CW and pulsed modes was obtained by comparing to the signal arising from the known thickness (25 μm) and density of isolated phosphorus donors (10^{14} cm^{-3}) in the epi-layer substrate. We estimate that the error in the spin count is at most about a factor of two. The spin-counting results for signals from natural dots are tabulated in Table I. We find that the total density of confined dots, as well as dots having a long T_2 , reduces by a factor of two upon changing the confinement temperature from 5 K to 10 K. Further, irrespective of the confining temperature, about 10 % of all the dots seen in the CW experiment show a long T_2 in pulsed ESR at 350 mK.

We measured the T_1 of only those dots that have a long T_2 , by using a $\tau = 1.6 \mu\text{s}$ between the second and third pulses of the 3-pulse experiment, to ensure that all spins with $T_2 = 0.8 \mu\text{s}$ have already decayed away. Currently, we have not measured the T_1 for electrons that showed a short T_2 . To extract T_1 , the echo intensity at the end of the 3-pulse sequence is plotted versus t and fit with an exponential recovery curve (Fig. 4). Note that in an ideal inversion recovery experiment, the echo signal at short

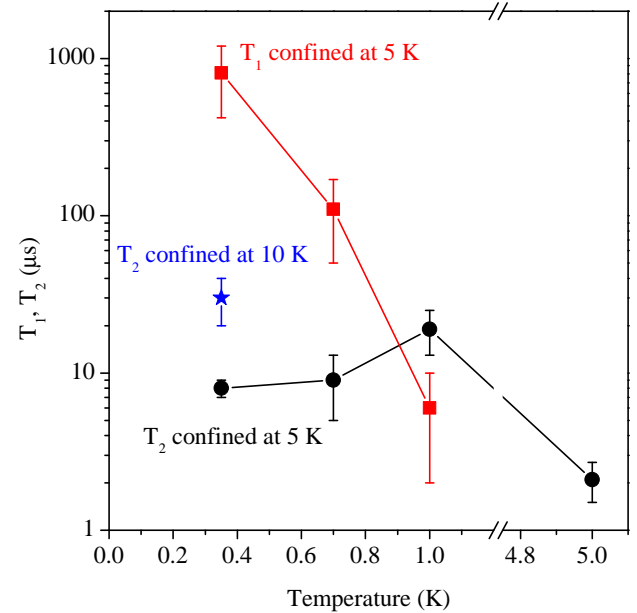


FIG. 5. T_1 and T_2 as a function of temperature for natural dots that show a long T_2 . Squares and circles correspond to natural dots confined at 5 K, while the star shows the T_2 for dots confined at 10 K and measured at 350 mK. Lines are guides for the eye.

TABLE II. Gate voltage dependence of T_1 , T_2 and T_2^* .

V_G (V)	T (K)	T_1 (μs)	T_2 (μs)	T_2^* (μs)
0 (confined at 5 K)	0.35	800 ± 400	8 ± 1	0.3
2 (mobile)	5.0	0.33 ± 0.05	0.39 ± 0.04	0.3

t ($t \leq T_1 \ln(2)$) should be negative, corresponding to an inversion of the spins by the initial π pulse. In our experiment, non-ideality of the inversion pulse due to the small microwave field B_1 (\sim ESR linewidth) and its inhomogeneity across the sample, precludes us from observing a negative echo signal. Therefore, the intensity of the echo is fit by the exponential dependence ($a - b \exp\{-t/T_1\}$) to find the characteristic time T_1 .

Table II summarizes the gate voltage dependence of T_1 , T_2 and T_2^* contrasting natural quantum dots confined at 5 K with mobile electrons. Fig. 5 summarizes the temperature dependence of T_1 's and T_2 's of natural dots when confined at 5 K and 10 K.

IV. DISCUSSION

Mobile electrons ($V_G = 2 \text{ V}$) have sub-microsecond T_1 and T_2 at 5 K, an order of magnitude shorter than the relaxation times measured for 2D electrons in high-mobility Si/SiGe heterostructures⁸. As in Si/SiGe structures, T_1 and T_2 relaxation may be caused by a fluctuating Rashba effective magnetic field arising from the spin-orbit cou-

pling^{9,10}. Alternatively, other spin relaxation processes also arising from spin-orbit coupling such as the Elliott-Yafet mechanism^{16–18} could result in short T_1 's and T_2 's especially in low mobility structures¹⁹ like a MOSFET. While a detailed understanding of the process causing spin relaxation of mobile 2D electrons remains a topic for future work, for now spin relaxation can be plausibly associated with spin-orbit coupling modulated by mobile electron scattering.

Upon confining 2D electrons into quantum dots and cooling to low enough temperature, theory¹² predicts that the Rashba field should become less effective in inducing relaxation and therefore longer T_1 and T_2 should emerge. In agreement, our results as summarized in Table II ($V_G = 0$ V) and Fig. 5 show that T_1 for natural dots confined at 5 K rises with decreasing temperature reaching 0.8 ms at 350 mK. While the detailed functional form of T_1 seen in Fig. 5 is unclear, the fact that T_1 rises as temperature decreases is in line with trends expected for phonon related mechanisms. Our results are qualitatively in agreement with recent experiments on small (200 nm lithographic dimensions) dots in silicon structures^{6,7}, demonstrating that T_1 is controlled by inelastic phonon scattering and that this scattering can be suppressed at lower temperatures, leading to $T_1 \sim 1$ s at 48 mK. More temperature points and a study of T_1 as a function of confinement energy need to be added to the data in Fig. 5 in order to make quantitative comparisons to the theory and other experiments. However for now, the T_1 data show that by confining 2D electrons into quantum dots with a few millivolts binding energy and cooling to low enough temperatures (350 mK), Rashba field fluctuations are made less effective and T_1 can be increased by almost four orders of magnitude.

Restricting electron motion also increases T_2 (Fig. 5). After confining into quantum dots at 5 K, the spins have a T_2 of around 2 μ s at 5 K, which is about five times longer than mobile 2D electrons. Upon cooling, T_2 increases to around 20 μ s at 1 K where as seen in Fig. 5, it is comparable to T_1 . Therefore at 1 K, T_2 is limited by the energy relaxation mechanisms that control T_1 ($T_2 \sim T_1$). T_2 appears to decrease on further cooling to around 10 μ s at 350 mK (error bars are 67% confidence bounds). Significantly, T_2 is two orders of magnitude less than T_1 at 350 mK. The fact that $T_2 \ll T_1$ at 350 mK demonstrates that T_2 is not limited by T_1 relaxation but instead the spins decohere by a different, extrinsic mechanism.

We can rule out fluctuating hyperfine interactions due to nuclear spins² as the extrinsic mechanism limiting coherence at 350 mK. This extrinsic process limits the Hahn echo T_2 in individual GaAs quantum dots from a few μ s^{20,21} to 30 μ s²², much shorter than T_1 . However, similar processes cannot explain the 10 μ s T_2 measured in our device since it is fabricated on an isotopically enriched ²⁸Si substrate having a negligible number of nuclear spins (800 ppm ²⁹Si fraction).

A clue to the mechanism controlling T_2 is provided by the apparent increase in T_2 from 350 mK to 1 K. Such

an increase of T_2 with temperature is reminiscent of motional narrowing of a decoherence mechanism involving interactions between spins. The exchange coupling provides one possible mode for such an interaction. Simple estimates of the wavefunction overlap and the exchange interaction between neighboring dots can be made for electrons confined at 5 K where the confinement energy is at least about 4 meV (Fig. 1(c)) and the distance between dots is about 90 nm (dot density of 1.2×10^{10} cm⁻²). With these parameters and a simple quartic confining potential²³, one calculates an exchange of about 300 kHz, in the same range as $1/T_2$. Precise agreement is not expected as the exchange is exponentially sensitive to the dot spacing and depth. This idea that exchange between neighboring dots controls T_2 is also supported by the longer T_2 observed when the dots are confined at 10 K (Fig. 5) since the lower electron density implies a larger distance between dots and consequently smaller exchange coupling. Further, in practice there will be a broad distribution of exchange between dots in the sample; this distribution in exchange could account for the variation in T_2 seen in Fig. 2(b) and Fig. 3. A fluctuating exchange between dots appears to be the likely extrinsic decoherence mechanism that is causing $T_2 \ll T_1$.

V. CONCLUSION

We have shown that for electrons confined in natural quantum dots having a few millivolts of confinement energy, T_1 reaches almost a millisecond and the longest T_2 is about 30 μ s at 350 mK. On the other hand, mobile 2D electrons have short T_1 and T_2 of about 0.3 μ s, possibly controlled by a Rashba field. Our results confirm that confinement makes Rashba fluctuations less effective leading to a four order of magnitude longer T_1 in isolated quantum dots at the Si/SiO₂ interface, similar to GaAs quantum dots and many-electron dots in Si/SiGe and Si/SiO₂ heterostructures. Recently there has been encouraging progress towards a scalable quantum computing architecture using gated dots in Si/SiGe²⁴ and Si/SiO₂²⁵ systems. The long T_1 we measure in silicon quantum dots suggest that these schemes have a promising future.

While the natural dots show a T_2 about one to two orders of magnitude longer than mobile electrons, the T_2 is still significantly shorter than T_1 . This shorter T_2 is likely due to exchange interactions between neighboring dots, an explanation which is consistent with estimates and the experimental observation of a threefold increase in T_2 at lower electron density. The lowest electron density (0.5×10^9 cm⁻²) in this work is at the limit of the sensitivity of our ESR spectrometer. Experiments which eliminate the exchange effects will require improved sensitivity.

ACKNOWLEDGMENTS

This work was supported by the NSF through the Princeton MRSEC (DMR-0819860) and by NSA/LPS

and ARO through the University of Wisconsin (W911NF-08-1-0482).

^{*} Current address : Applied Physics Dept., Yale University, New Haven, CT 06511, USA; shyam.shankar@yale.edu

¹ D. Loss and D. P. DiVincenzo, Phys. Rev. A, **57**, 120 (1998); R. Vrijen, E. Yablonovitch, K. Wang, H. W. Jiang, A. Balandin, V. Roychowdhury, T. Mor, and D. DiVincenzo, *ibid.*, **62**, 012306 (2000); M. Friesen, P. Rugheimer, D. E. Savage, M. G. Lagally, D. W. van der Weide, R. Joynt, and M. A. Eriksson, Phys. Rev. B, **67**, 121301 (2003).

² R. Hanson, L. P. Kouwenhoven, J. R. Petta, S. Tarucha, and L. M. K. Vandersypen, Rev. Mod. Phys., **79**, 1217 (2007).

³ D. P. DiVincenzo, Fortsch. Phys.-Prog. Phys., **48**, 771 (2000).

⁴ G. Feher and E. A. Gere, Phys. Rev., **114**, 1245 (1959); J. P. Gordon and K. D. Bowers, Phys. Rev. Lett., **1**, 368 (1958); M. Chiba and A. Hirai, J. Phys. Soc. Jpn, **33**, 730 (1972).

⁵ Recent unpublished results. A. M. Tyryshkin, S. A. Lyon, S. Tojo, K. M. Itoh, J. J. L. Morton, M. L. W. Thewalt, H. Riemann, N. V. Abrosimov, P. Becker, H.-J. Pohl, (unpublished). The longest published T_2 is 60 ms at 7 K. See A. M. Tyryshkin, S. A. Lyon, A. V. Astashkin, and A. M. Raitsimring, Phys. Rev. B, **68**, 193207 (2003).

⁶ R. R. Hayes, A. A. Kiselev, M. G. Borselli, S. S. Bui, E. T. Croke, P. W. Deelman, B. M. Maune, I. Milosavljevic, J.-S. Moon, R. S. Ross, A. E. Schmitz, M. F. Gyure, and A. T. Hunter, (2009), arXiv:0908.0173 [cond-mat].

⁷ M. Xiao, M. G. House, and H. W. Jiang, Phys. Rev. Lett., **104**, 096801 (2010).

⁸ A. M. Tyryshkin, S. A. Lyon, W. Jantsch, and F. Schäffler, Phys. Rev. Lett., **94**, 126802 (2005).

⁹ Y. A. Bychkov and E. I. Rashba, J. Phys. C, **17**, 6039 (1984).

¹⁰ C. Tahan and R. Joynt, Phys. Rev. B, **71**, 075315 (2005).

¹¹ S. Shankar, A. M. Tyryshkin, S. Avasthi, and S. A. Lyon, Physica E, **40**, 1659 (2008).

¹² A. V. Khaetskii and Y. V. Nazarov, Phys. Rev. B, **64**, 125316 (2001).

¹³ A. Schweiger and G. Jeschke, *Principles of Pulse Electron Paramagnetic Resonance* (Oxford University Press, Oxford, 2001).

¹⁴ T. Ando, A. B. Fowler, and F. Stern, Rev. Mod. Phys., **54**, 437 (1982).

¹⁵ The calculation is based on an approach developed in C. S. Jenq, *High field generation of interface states and electron traps in MOS capacitors*, Ph.D. thesis, Princeton University (1978). For details see S. Shankar, *Electron spin coherence in bulk silicon and silicon heterostructures*, Ph.D. thesis, Princeton University (2010).

¹⁶ R. J. Elliott, Phys. Rev., **96**, 266 (1954).

¹⁷ Y. Yafet, "Solid state physics," (Academic Press, 1963) p. 1.

¹⁸ J. L. Cheng, M. W. Wu, and J. Fabian, Phys. Rev. Lett., **104**, 016601 (2010).

¹⁹ Z. Wilamowski and W. Jantsch, Phys. Rev. B, **69**, 035328 (2004).

²⁰ J. R. Petta, A. C. Johnson, J. M. Taylor, E. A. Laird, A. Yacoby, M. D. Lukin, C. M. Marcus, M. P. Hanson, and A. C. Gossard, Science, **309**, 2180 (2005).

²¹ F. H. L. Koppens, K. C. Nowack, and L. M. K. Vandersypen, Phys. Rev. Lett., **100**, 236802 (2008).

²² H. Bluhm, S. Foletti, I. Neder, M. Rudner, D. Mahalu, V. Umansky, and A. Yacoby, (2010), arXiv:1005.2995 [cond-mat].

²³ G. Burkard, D. Loss, and D. P. DiVincenzo, Phys. Rev. B, **59**, 2070 (1999).

²⁴ C. B. Simmons, M. Thalakulam, B. M. Rosemeyer, B. J. V. Bael, E. K. Sackmann, D. E. Savage, M. G. Lagally, R. Joynt, M. Friesen, S. N. Coppersmith, and M. A. Eriksson, Nano Letters, **9**, 3234 (2009).

²⁵ E. P. Nordberg, G. A. T. Eyck, H. L. Stalford, R. P. Muller, R. W. Young, K. Eng, L. A. Tracy, K. D. Childs, J. R. Wendt, R. K. Grubbs, J. Stevens, M. P. Lilly, M. A. Eriksson, and M. S. Carroll, Phys. Rev. B, **80**, 115331 (2009).